Journal of Siberian Federal University. Mathematics & Physics 2009, 2(3), 258–270

УДК 519.684.4, 550.394.2

Fast Modelling of Tsunami Wave Propagation at PC by Hardware Computer Code Acceleration

Mikhail M.Lavrentiev *
Institute of Automation and Electrometry,
Siberian Branch of RAS,
Koptyga 1, Novosibirsk, 630090
Russia

Andrey G.Marchuk †
Institute of Computational Mathematics
and Mathematical Geophysics,
Siberian Branch of RAS,
pr. Lavrent'eva 6, Novosibirsk, 630090
Russia

Received 10.05.2009, received in revised form 10.06.2009, accepted 20.06.2009

The field programmable gates array (FPGA) microchip is applied to achieve valuable performance gain calculating of tsunami wave propagation at modern regular personal computer. The two-step MacCormack scheme was used for numerical approximation of the shallow water system. After a number of numerical tests, the authors describe the idea of PC-based tsunami wave propagation simulation. Comparison with the available analytic solutions and with the reference code show pretty good precision of the developed software application. It takes less then 1 *minute to compute* 1 *hour of the wave propagation in* 3000×2500 *nodes computation domain. Using the nested greed approach, it is possible to move from about* 300 *meters step calculation mesh to the one with* 10 *m step. Using the proposed Calculator, the entire computation process (to calculate the wave propagation from the source area to the coast) takes about* 2 *min. The distribution of tsunami wave maximal heights along the coast of the Southern part of Japan is given as an example. In particular, dependence of wave maximal heights on particular location of tsunami source is investigated. Model* 100×200 *km sources have a realistic parameters corresponding to this region. As is observed numerically, only selected parts of the entire coast line are subject to dangerous tsunami wave amplitude. However, extreme tsunami heights at some of those areas can be attributed to local bathymetry. The proposed hardware acceleration to compute tsunami wave propagation can be used for rapid (say, in a few minutes) tsunami danger evaluation for a particular village or industrial unit at the coast.*

Keywords: numerical modelling, tsunami wave propagation, computer code acceleration.

Timely reporting of a dangerous tsunami wave at a particular coastal zone location is critically important to reduce human losses and to minimize possible impact to economy for the so-called near field tsunamis. Unfortunately, the problem of well-timed warning about the tsunami wave danger in this case (after the major offshore earthquake) is still unresolved, even if the number of publications is rather large, see, for example, [1]. In case of the seismic event offshore Japan,

*mmlavrentiev@gmail.com
†mag@omzg.sscc.ru

tsunami wave approaches the nearest dry land in approximately 20 minutes. It means that one has just a few minutes for analysis to provide authorities with evaluation of the expected tsunami wave danger. In case of the strong earthquake the electric power supply shut down is possible, so it would be better not to use supercomputer facilities. The authors are using advantages of the modern computer architectures to accelerate numerical simulation of tsunami wave propagation. Specialized FPGA (Field Programmable Gates Arrays) based Calculator have been developed and tested. Based on a number of numerical tests we demonstrate the advantages of the new super rapid method for modeling of tsunami wave propagation. In the present paper we briefly describe the proposed approach and show the numerical results, obtained in the recent years.

Our point is to use just the regular modern Personal Computer (PC) and to achieve valuable performance gain exploiting Graphic Processing Units (GPUs) and FPGAs as co-processors. So, we propose a specific hardware configuration and the corresponding modelling code.

Robust evaluation of tsunami wave danger should be based on correct process simulation: wave generation, wave propagation, and inundation of a dry land. In the study we deal with the stages of wave formation and its following propagation only, in order to make the computations faster, at the same time keeping a sufficient accuracy. So, we suppose that the tsunami wave is caused by a certain disturbance of a sea surface. This initial disturbance serves as the initial conditions in the governing evolution type equations (shallow water system, in fact). We also do not touch the inundation mapping questions. Therefore, we do not compute a wave at small depths (below 5 m) where we suggest reflection type boundary conditions at such depth to estimate the wave height in the near-shore area and to account reflected waves. At the parts of the boundary, which separate our computational domain from the ocean, we use conditions for free passage of the wave out of the domain. There are several software tools to calculate the wave propagation over the real digital bathymetry, see [2–6].

Among the most popular software instruments the MOST (Method of Splitting Tsunamis) software package should be mentioned. This official instrument of the USA NOAA tsunami warning centers for simulation of all tsunami phases – generation, propagation, and inundation of the dry land, [2,4]. Calculation of the wave propagation over the chosen water area is based on numerical solution of linear or nonlinear shallow water differential equations.

Alternatively, we implement he two half-step Mac-Cormack scheme for numerical approximation of the shallow water system [7,8]. Comparison with the exact solution (in special cases of sea bed relief) shows a very good precision of the method in use [9,10]. It shows better tracking of the wave front against the MOST software.

A number of numerical tests using the real digital bathymetry offshore Japan and Kamchatka Peninsula prove that it takes about 50 sec to solve numerically the shallow water system at the 10^7 nodes computational domain [11,12]. Nested grid approach has been also tested [13,14].

1. Mathematical Statement of the Problem

The referred software package MOST (like many other tools) uses the following equivalent form of a shallow water system (which does not take into account such external forces as sea bed friction, Coriolis force and others), which could be found in [4]:

$$\frac{\partial H}{\partial t} + \frac{\partial uH}{\partial x} + \frac{\partial vH}{\partial y} = 0,$$

$$\frac{\partial u}{\partial t} + u\frac{\partial u}{\partial x} + v\frac{\partial u}{\partial y} + g\frac{\partial H}{\partial x} = g\frac{\partial D}{\partial x}, \tag{1}$$

$$\frac{\partial v}{\partial t} + u\frac{\partial v}{\partial x} + v\frac{\partial v}{\partial y} + g\frac{\partial H}{\partial y} = g\frac{\partial D}{\partial y},$$

where $H(x,y,t) = \eta(x,y,t) + D(x,y,t)$ is the entire height of water column, $\eta(x,y,t)$ being the sea surface disturbance (wave height), $D(x,y)$ – depth (which is supposed to be known at all grid points), u and v components of water flow velocity vector, g – acceleration of gravity.

The system of shallow-water equations can be solved using the difference scheme. In this case values of tsunami wave parameters $\eta(x,y,t)$, u, and v are defined in nodes of the regular grid linked to geographical coordinates. In the beginning, in all grid nodes the initial condition of a media is set. For example, everywhere besides the source area, the values of the grid variables η^0_{ij}, u^0_{ij}, v^0_{ij}, $(i = 1,\dots,N,\ j = 1,\dots,M)$ are equal to zero. Further, according to the difference scheme approximating, the system of differential equations (1), the wave parameters η^n_{ij}, u^n_{ij}, v^n_{ij} at the grid nodes on subsequent time layers $t^n = n\tau$, are calculated. Here, the value of the time step τ is usually determined from the stability condition, the physical meaning of which is the inadmissibility of the wave moving by more than one spatial step (Δx or Δy) in one time step.

The shallow water equations (1) at the mesh nodes on the n-th time step will be approximated with the help of explicit two–steps Mac–Cormack finite difference scheme of the second order approximation [15]:

First half-step:

$$\begin{aligned}
&\frac{\hat H^{n+1}_{ij} - H^n_{ij}}{\tau} + \frac{H^n_{ij}u^n_{ij} - H^n_{i-1j}u^n_{i-1j}}{\Delta x} + \frac{H^n_{ij}v^n_{ij} - H^n_{ij-1}v^n_{ij-1}}{\Delta y} = 0,\\
&\frac{\hat u^{n+1}_{ij} - u^n_{ij}}{\tau} + u^n_{ij}\frac{u^n_{ij} - u^n_{i-1j}}{\Delta x} + v^n_{ij}\frac{u^n_{ij} - u^n_{ij-1}}{\Delta y} + g\frac{\eta^n_{ij} - \eta^n_{i-1j}}{\Delta x} = 0,\\
&\frac{\hat v^{n+1}_{ij} - v^n_{ij}}{\tau} + u^n_{ij}\frac{v^n_{ij} - v^n_{i-1j}}{\Delta x} + v^n_{ij}\frac{v^n_{ij} - v^n_{ij-1}}{\Delta y} + g\frac{\eta^n_{ij} - \eta^n_{ij-1}}{\Delta y} = 0.
\end{aligned} \tag{2}$$

Second half-step:

$$\begin{aligned}
&\frac{H^{n+1}_{ij} - (\hat H^{n+1}_{ij} + H^n_{ij})/2}{\tau/2} + \frac{\hat H^{n+1}_{i+1j}\hat u^{n+1}_{i+1j} - \hat H^{n+1}_{ij}\hat u^{n+1}_{ij}}{\Delta x} + \frac{\hat H^{n+1}_{ij+1}\hat v^{n+1}_{ij+1} - \hat H^{n+1}_{ij}\hat v^{n+1}_{ij}}{\Delta y} = 0,\\
&\frac{u^{n+1}_{ij} - (\hat u^{n+1}_{ij} + u^n_{ij})/2}{\tau/2} + u^n_{ij}\frac{\hat u^{n+1}_{i+1j} - \hat u^{n+1}_{ij}}{\Delta x} + v^n_{ij}\frac{\hat u^{n+1}_{ij+1} - \hat u^{n+1}_{ij}}{\Delta y} + g\frac{\hat\eta^{n+1}_{i+1j} - \hat\eta^{n+1}_{ij}}{\Delta x} = 0,\\
&\frac{v^{n+1}_{ij} - (\hat v^{n+1}_{ij} + v^n_{ij})/2}{\tau} + u^n_{ij}\frac{\hat v^{n+1}_{i+1j} - \hat v^{n+1}_{ij}}{\Delta x} + v^n_{ij}\frac{\hat v^{n+1}_{ij+1} - \hat v^{n+1}_{ij}}{\Delta y} + g\frac{\hat\eta^{n+1}_{ij+1} - \hat\eta^{n+1}_{ij}}{\Delta y} = 0.
\end{aligned} \tag{3}$$

Here $\hat F^{n+1}_{ij}$ presents intermediate values of wave parameters after the first time half-step.

Usually, the real tsunami wave simulation is performed in a spherical or geodetic coordinate system (λ,ϕ), where λ is the longitude and ϕ is the latitude in arc degrees. Accordingly, the following relations are used to calculate the differences Δx and Δy:

$$\Delta x_{ij} = \frac{\pi(\lambda_{i+1} - \lambda_i)}{180^\circ} R_E \cos(\phi_i), \quad \Delta y_{ij} = \frac{\pi(\phi_{i+1} - \phi_i)}{180^\circ} R_E,$$

where R_E stands for the Earth radius. This scheme looks similar to the splitting method (with respect to space variables), which is used in the referred MOST software package. Indeed, in order to calculate the values of the sought functions at grid-point $(i,j,n+1)$ the values at 3 points of the previous time step, (i,j,n), $(i-1,j,n)$, and $(i,j-1,n)$ are used during the first

half-step in (2), and the values at the points (i, j, n), $(i+1, j, n)$, and $(i, j+1, n)$ are used during the second half-step in (3). Comparison of the known analytic solutions with the numerically obtained ones show that the proposed attempt to realize the three-points calculation stencil (Mac-Cormack scheme) seems to be preferable compared to the one from the MOST software package [9,10]

2. FPGA Based Calculator

In order to achieve performance gain, the FPGA-based Calculator has been designed.

To enjoy advantages of the FPGA microchip features, the stream processor architecture was proposed for this algorithm implementation. The proposed Calculator contains several processor elements (PEs). Each of these elements performs a pipeline with a sequential data stream. "On board" memory contains all the necessary information. The calculation speed-up by FPGA architecture is based on the inner memory (BRAM) access for implementing stencil buffer.

The Calculator architecture makes it possible to process several nodes in parallel. At the same time, the user can connect a number of PEs to make several iterations. So, the computation pipeline could be optimized accounting features of the FPGA microchip in use. Mac-Cormack finite difference approximation fits very well with the Calculator architecture processing 1 node at one computer clock cycle.

The originally designed in hardware "Calculator", based of FPGA microchip Xilinx Virtex-7 VC709, was used for numerical tests, see [7,8] for details.

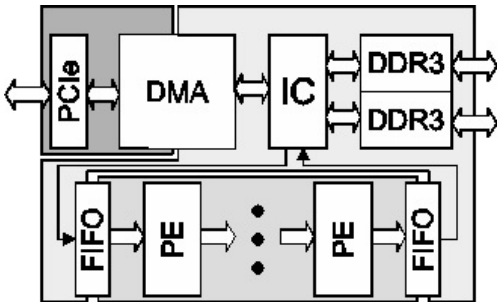

Figure 1. Calculator architecture. For the FPGA algorithm implementation architecture of the stream processor was proposed. It consists of a certain processor elements (PE). Such PE executes a version of 2-dimension run, a pipeline with a sequential data stream. In addition to the calculator itself, the processor has memory controllers DDR3, PCIe controller, and DMA module, responsible for the interaction between the calculator and the memory of the host computer. Such interaction is arranged as a direct memory access (DMA).

3. Comparison with Exact Solutions and Reference Code

In order to check reliability of results obtained by the described method, a number of numerical tests have been carried out. The first test consists of calculation of the tsunami wave propagation from a round source in an area with the sloping bottom topography. The water area of 1000×1000 km was considered, computational grid has equal steps in space variables, namely $\Delta x = \Delta y = 1000$m. The center of the circular tsunami source with the radius of 50 km

was located in the middle of the region (horizontally) at the distance of 300 km from the lower boundary, where the depth was vanishing. In the rest of the computational domain, the depth linearly increased according to the formula $D(x, y) = 0.01y$, where y is the distance to the lower boundary of the region. The initial vertical displacement h of the tsunami source is determined by the formula

$$h(r) = 1 + \cos\left(\frac{\pi r}{r_0}\right), \qquad 0 \leqslant r \leqslant r_0. \tag{4}$$

Here, the parameter r presents the distance to the center of the considered source of radius r_0. Thus, in the center of the source area, the initial displacement of the water surface was +2 m. This source generated a circular wave having a height of 0.95 m at a distance of 50 km from the center. It was such a wave height that was used at the initial circular wave front with the radius of 50 km in the course of estimating the wave amplitude at all points of the region according to the ray approximation [17,18]. This distribution of tsunami wave amplitude (given in an analytic form) was compared with the same distributions obtained by numerically modelling of the tsunami propagation using the MOST software and the proposed Mac-Cormack algorithm (Figure 2).

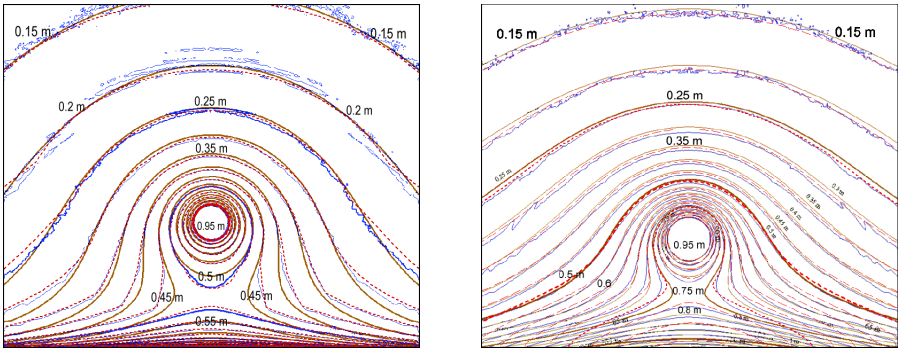

Figure 2. *Left*: Isolines of maximal wave heights distribution above bottom slope obtained by: exact solution to shallow water system [17,18] (brown lines), numerical solution with the FPGA based Calculator (red dashed lines), and using the MOST software package (blue lines). The offshore distance is measuring along vertical axis relative to the figure's bottom boundary. *Right*: Isolines of maximal wave heights distribution above the parabolic bottom topography [16], obtained by: the wave-ray solution to shallow water system (grey lines), numerical solution with the FPGA based Calculator (dashed lines), and using the MOST package (black lines). The offshore distance is measuring along vertical axis relative to the figure's bottom boundary.

Figure 2 (left) shows that at sufficiently large depths (exceeding 500 m), the contours of all three distributions of tsunami height maxima are quite close to each other. The proximity of the results of numerical calculations for the two algorithms under consideration is also preserved near the coast. The increased difference in comparison of numerical and wave-ray approach results in the coastal zone is caused by the neglection of the effect of increasing wave height due to reflection from the coast.

Another numerical test was similar to the first one and consider the case of a parabolic bottom relief. Consider the same computational area of 1000×1000 km with a computational grid having spatial steps $\Delta x = \Delta y = 1000$ m. The center of the circular source with 50 km radius was also located in the middle of the area at a distance of 300 km from the lower boundary, where the

depth is equal to zero. In the rest of the computational domain, the depth increased according to the formula $D(x, y) = 10^{-8}y^2$, where y is the distance to the lower boundary of the region. The initial vertical displacement inside the circular source is determined by the formula (4). Figure 2 (right) presents, similarly to the Figure 2 (left), the isolines of the distributions of tsunami height maxima calculated by the MOST and Mac-Cormack algorithms, as well as the estimates of these maxima in the framework of the ray model [16].

From the Figure 2 (right), similarly as from the Figure 2 (left), it follows that at sufficiently large depths (more than 200 m), the contours of all three distributions (obtained numerically by MOST and Mac-Cormack algorithms and distribution of the wave-ray solution) of tsunami height maxima are quite close to each other. Here, the similarity of the results of numerical calculations by the two algorithms under consideration is observed up to the coastline itself (the lower boundary of the region), while there is an increase in the difference between these results in the coastal zone with estimates by the wave-ray approximation.

Based on the results of calculations of the wave propagation over a bottom slope, the correctness of the wave front kinematics modelling by the two numerical methods considered is also estimated. Figure 3 shows the comparison of the wave front position with an interval of 5 minutes calculated according to the McCormack scheme with the exact solution of the kinematic problem at the same time points. In order to prevent the points from merging (as it happens at the initial moment), the moments of output of the points of the calculated wave front are taken 3 seconds later than the moment of the corresponding exact solution of the kinematic problem [17,18]. We do not present the wave front positions as a result of numerical simulations of the tsunami according to the MOST software, since the positions of the front points exactly coincide with the positions of the corresponding points as a result of the numerical calculation of the wave dynamics using the McCormack scheme.

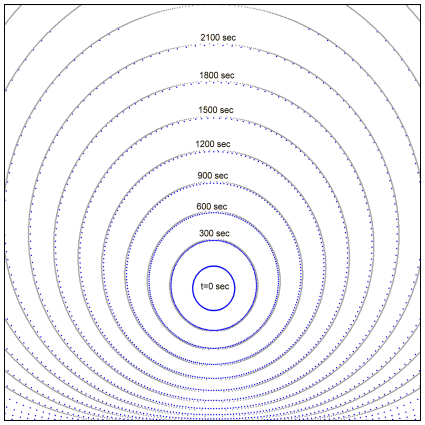

Figure 3. Comparison of the tsunami wave isochrones over the sloping bottom: obtained by numerical experiments with MOST and Mac-Cormack algorithms (grey lines) and exact solution (black points).

The last “comparison” numerical test was carried out in order to verify the correctness of modelling the reflection of a wave from a completely reflecting boundary located at an angle of 45 degrees to the direction of motion of the flat wave front. In a rectangular 1000×2000 nodes computational domain, a long wave about 1 m height generated by a one-dimensional source parallel to the lower boundary of the region propagates over the region and is reflected from the

inner boundary extending from the right boundary (upper right corner) to the left one at an angle of 45 degrees to ordinate axis (Figure 4).

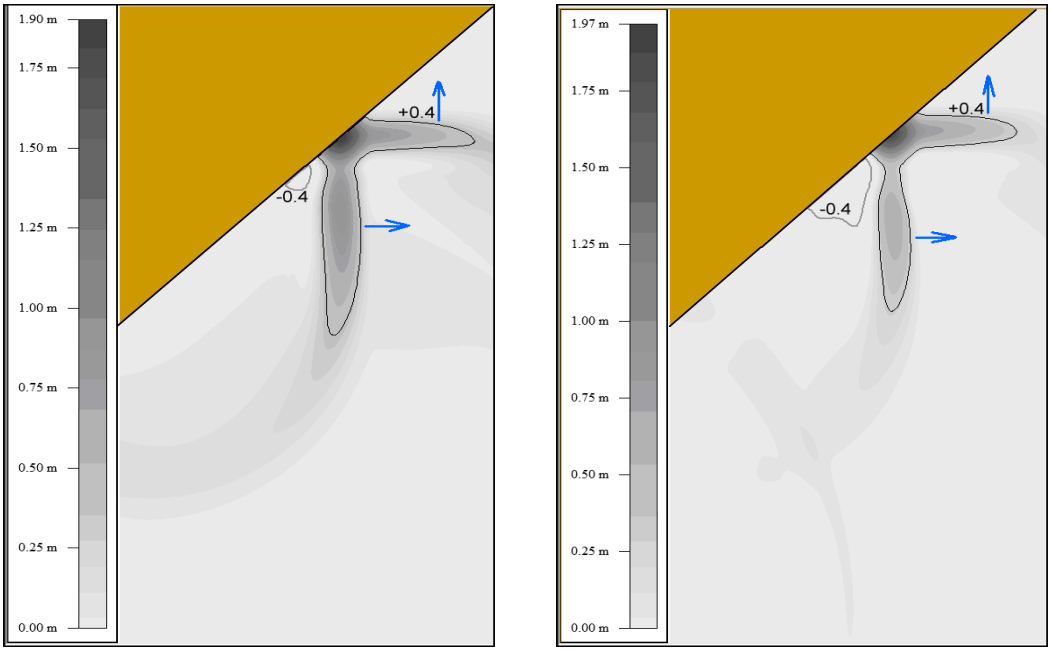

Figure 4. Water surface after $3,000$ sec of calculation using the Mac-Cormack scheme at FPGA (left figure) and using the MOST approach (right figure). Thin black line indicates the 0.4 m isoline, while the gray line shows -0.4 m isoline.

Figure 4 shows the distribution of the vertical displacement of the water surface in the entire region calculated using the Mac-Cormack difference scheme (left figure) and the MOST algorithm (right figure). The dark line shows the tsunami height isoline corresponding to the value of 0.4 m. The grey line outlines the water area with the surface displacement less then $-0,4$ m. Both figures confirm the correctness of numerical modelling of the process of wave reflection from a completely reflecting boundary. It is clear from the figures that the direction of motion of the reflected wave in both cases is orthogonal to the direction of the incident wave.

4. Distribution of Maximal Wave Heights Along the Shoreline

The acceleration of numerical calculations of the tsunami propagation is required, first of all, by tsunami warning services to fast estimate the expected wave height at different points on the coastline. Therefore, this estimation is required before tsunami wave attacks the shore. This section will demonstrate the ability of the proposed software to solve this problem in the area with real bathymetry within a few tens of seconds.

The series of numerical experiments were arranged at the gridded bathymetry around Kii Peninsula and Shikoku Island (southern part of Japan), developed on a base of Japanese bathymetric data produced by the Japan Oceanographic Data Center (JODC) (see [19]), presented in Figure 5.

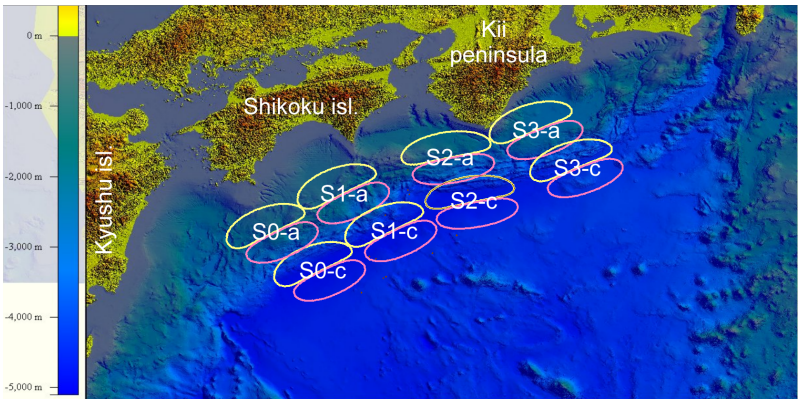

Figure 5. Digital bathymetry around Kii Peninsula and Shikoku Island (Japan). Positions of model tsunami sources are indicated.

The above bathymetry and the computational grid have the following characteristics:

(1) Gridded area size is 3000×2496 nodes; **(2)** Grid steps are 0.003 and 0.002 degrees (which means 280.6 and 223 meters, respectively); **(3)** Array covers the area between 131° and 140° E, 30.01° and 35° N; **(4)** Time step used in computations is equal to 0.5 sec.

The shape and profile of model tsunami sources (used in numerical experiments) are based on the available geological and geophysical information. Due to this, the typical for subduction zone seabed displacement area for 8.0 M earthquake was approximated by 100×200 km rectangle having maximum height as 300 cm. The initial seabed displacement at such a model source is shown in Figure 6.

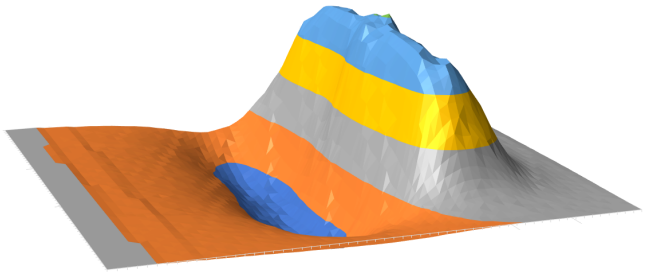

Figure. 6. 3D image of the model tsunami source, used for numerical modelling.

Position and shapes of the sources used for tsunami modelling are shown in Figure 5, where geography of the computational domain is also presented. In this figure only the closest to a coast sources $S_i - a$ $(i = 1, \ldots 4)$ and more distant to a coast ones $S_i - c$ $(i = 1, \ldots 4)$ are indicated. Their positive parts are shaped by pink color, and negative parts (water surface depression) are outlined by yellow color. Intermediate sources $S_i - b$ $(i = 1, \ldots 4)$ are situated between sources $S_i - a$ and $S_i - c$.

The distributions of the wave height maxima in the entire area generated by some model sources are presented in Figures 8(A)–8(D). In the right part of each drawing the legend for color-height relation is presented.

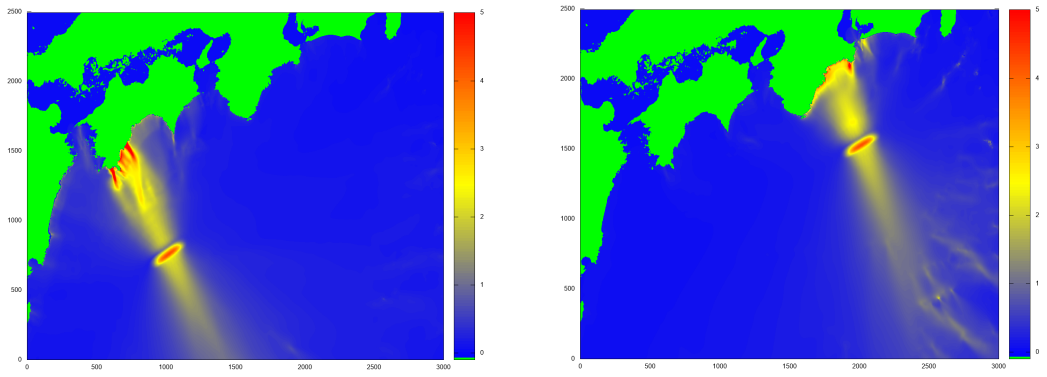

Figure 7. Calculated height maxima in entire computational domain from tsunami wave, generated by the source $S_0 - c$ (left) and $S_3 - b$ (right), see Figure 3.

As is observed from the Figure 7 (left), the same shape of the initial sea surface displacement causes the tsunami wave heights of up to 6 m at certain areas of the Kii Peninsula coast. At the same time, the Shikoku Island and the Kyushu Island coasts are practically safe with wave heights limited by 0.5 m. Otherwise, the source located opposite Kii peninsula seriously affected only its coast and is hazardless for Shikoku Island, see the Figure 7 (right).

Another kind of important information for tsunami warning is the computed distribution of tsunami wave maxima along the shoreline. Figures 8(A) and 8(D) shows such graphs for 6 model sources $S_0 - a, b, c$ and $S_3 - a, b, c$. We carried out numerical experiments for the same shape of initial see surface displacement (given in Figure 6), varying its position of such model source along shore and the distance of the model source from the shore. Colours of the wave maxima correspond to such distance. Numbers along the horizontal axis indicate the horizontal indexes of coastal computational grid points.

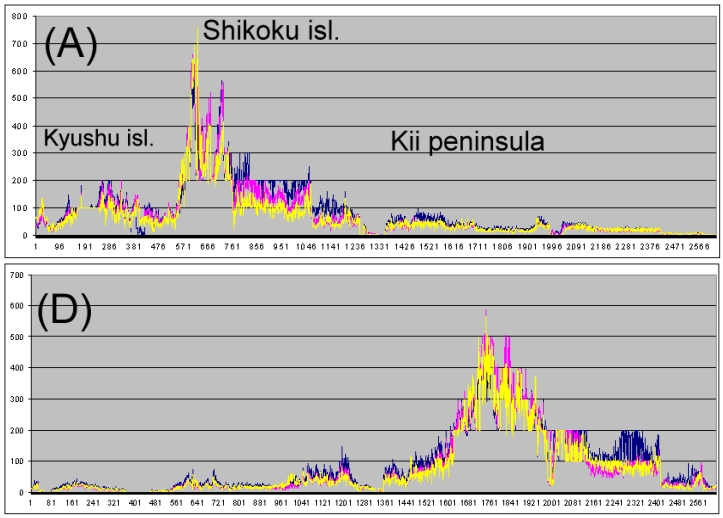

Figure 8. Distribution of tsunami wave maxima along the shore generated by the sources $S_0 - a, b, c$ (A) and $S_3 - a, b, c$ (D). Wave height maxima by $S_i - a$ sources are drawn as yellow lines, by $S_i - b$ sources – by blue lines, and by $S_i - c$ sources – by pink lines.

Let us say few words about digital bathymetry. The grid step used in our numerical experiments, being about 250 m, is considered too large these days. However, it length depends on the modelling goals. In case one needs a detailed evaluation of the expected wave heights along the entire shore line, it is necessary to carry out numerical modelling with the corresponding fine mesh size in the near-coastal regions. It could be done by choosing the properly small grid step in the whole water area. However, the number of computational nodes will increase by 2–3 orders, which results in the necessity of extended computational facilities or, alternatively, in a dramatic increase of the CPU time required for simulation. As for the proposed FPGA-based Tsunami Wave Calculator, the available memory resources dictate the limit of approximately 50 millions for a number of computational nodes.

The Calculator with a regular modern PC needs 25 sec to simulate wave propagation from the southern edge of the computational domain shown in Figure 5 to the shore. The "real" travel time for the wave is evaluated as 3200 sec. So, realization of Mac-Cormack difference scheme on FPGA hardware makes it possible to estimate expected wave height distribution along the coastline before tsunami arrival there.

5. Conclusion

In order to accelerate the calculation of tsunami wave propagation over the deep water area, a special FPGA based Calculator has been developed. The Mac-Cormack scheme was used for numerical solution to the shallow water system. Accuracy of the solution, obtained by the mentioned calculator, was tested by comparison with the known analytic solutions. The achieved precision is the same or better compared to the MOST software package. These results show the possibility of tsunami danger forecast in the real time mode.

Acknowledgement

This work was carried out under support of ICMMG SB RAS (state contract 0315-2019-0005) and IAE SB RAS.

References

[1] H.Tsushima and Y.Yusaku, Review on Near-Field Tsunami Forecasting from Offshore Tsunami Data and Onshore GNSS Data for Tsunami Early Warning, *J. Disaster Res.*, **9**(2014), no. 3, 339-357.

[2] E.Gica, M.Spillane, V.Titov, C.Chamberlin, and J.Newman, Development of the forecast propagation database for NOAA's short-term inundation forecast for tsunamis (SIFT), NOAA Technical Memorandum, 2008. URL: http://www.ndbc.noaa.gov/dart.shtml (access date: 15.06.2016).

[3] H.Kensaku, A.P.Vazhenin, A.G.Marchuk, Trans-Boundary Realization of the Nested-Grid Method for Tsunami Propagation Modeling, *Proceedings of the Twenty-fifth (2015) International Ocean and Polar Engineering Conference Kona, Big Island, Hawaii, USA*, **3**(2015), 741-747.

[4] V.Titov, F.Gonzalez, Implementation and testing of the method of splitting tsunami (MOST) model, NOAA Technical Memorandum ERL PMEL-112, 1997.

[5] N.Shuto, C.Goto, F.Imamura, Numerical simulation as a means of warning for near field tsunamis, *Coastal Engineering in Japan*, **33**(1990), no. 2, 173-193.

[6] A.C.Yalciner, B.Alpar, Y.Altinok, I.Ozbay, F.Imamura, Tsunamis in the Sea of Marmara: Historical Documents for the Past, Models for Future, *Marine Geology*, **190**(2002), 445-463.

[7] M.M.Lavrentiev, A.A.Romanenko, K.K.Oblaukhov, An.G.Marchuk, K.F.Lysakov, M.Yu.Shadrin, FPGA Based Solution for Fast Tsunami Wave Propagation Modeling, *The 27th International Ocean and Polar Engineering Conference*, (2017), 25-30 June, San Francisco, California, USA. P 924-929.

[8] M.M.Lavrentiev, K.F.Lysakov, An.G.Marchuk, K.K.Oblaukhov, and M.Yu.Shadrin, Hardware Acceleration of Tsunami Wave Propagation Modeling in the Southern Part of Japan, *Appl. Sci.*, **10**(2020), no. 12, 4159; https://doi.org/10.3390/app10124159

[9] M.M.Lavrentiev, An.G.Marchuk, K.K.Oblaukhov, and A.A.Romanenko, Comparative testing of MOST and Mac-Cormack numerical schemes to calculate tsunami wave propagation, *J. Phys.: Conf. Ser.*, (2020), 1666 012028; doi:10.1088/1742-6596/1666/1/012028

[10] M.M.Lavrentiev, A.A.Romanenko, K.K.Oblaukhov, An.G.Marchuk, K.F.Lysakov, M.Yu.Shadrin, Implementation of Mac-Cormack scheme for the fast calculation of tsunami wave propagation, *Oceans'17 MTS/IEEE, Aberdeen, June 19-22*, (2017).

[11] M.M.Lavrentiev, K.F.Lysakov, An.G.Marchuk, K.K.Oblaukhov, and M.Yu.Shadrin, Fast evaluation of tsunami waves heights around Kamchanka and Kuril Islands, *Science of Tsunami Hazards*, **38**(2019), no. 1, 1-13.

[12] M.Lavrentiev, K.Lysakov, An.Marchuk, K.Oblaukhov, M.Shadrin, FPGA-based Modelling of the Tsunami Wave Propagation at South Japan Water Area, *Proc. OCEANS'18 MTS/IEEE Kobe, Japan, May 28-31*, 2018.

[13] M.M.Lavrentiev, K.F.Lysakov, An.G.Marchuk, K.K.Oblaukhov, and M.Yu.Shadrin, FPGA Based Tsunami Wave Propagation Calculator, *J. Phys.: Conf. Ser.*, (2021), 1789 012011

[14] M.M.Lavrentiev, K.F.Lysakov, An.G.Marchuk, K.K.Oblaukhov, and M.Yu.Shadrin, FPGA based modeling of Tohoku tsunami using nested grids, *Proceedings of the Global Oceans 2020: Singapore - U.S. Gulf Coast*, October 5-14, 2020.

[15] R.W.MacCormack, A.J.Paullay, Computational Efficiency Achieved by Time Splitting of Finite–Difference Operators, *AIAA paper*, (1972), 72-154.

[16] An.G.Marchuk, Benchmark solutions for tsunami wave fronts and rays. Part 2: Parabolic bottom topography, *Science of Tsunami Hazards*, **36**(2017), no. 2, 70-85.

[17] An.G.Marchuk, Estimating Tsunami Wave Height over a Sloping Bottom in the Ray Approximation, *Numerical Analysis and Applications*, **8**(2015), no. 4, 304-313.

[18] An.G.Marchuk Benchmark solutions for tsunami wave fronts and rays. Part 1: sloping bottom topography. *Science of Tsunami Hazards*, **35**(2016), no. 2,

[19] $https://jdoss1.jodc.go.jp/vpage/depth500_file.html$